

# Hyperpolarization

## Effective PHIP Labeling of Bioactive Peptides Boosts the Intensity of the NMR Signal\*\*

Grit Sauer, Daichi Nasu, Daniel Tietze,\* Torsten Gutmann, Simon Englert, Olga Avrutina, Harald Kolmar,\* and Gerd Buntkowsky\*

**Abstract:** A series of novel bioactive derivatives of the sunflower trypsin inhibitor-1 (SFTI-1) suitable for hyperpolarization by parahydrogen-induced polarization (PHIP) was developed. The PHIP activity was achieved by labeling with L-propargylglycine, O-propargyl-L-tyrosine, or 4-pentynoic acid. <sup>1</sup>H NMR signal enhancements (SE) of up to a factor of 70 were achieved in aqueous solution. We found that an isolated spatial location of the triple bond within the respective label and its accessibility for the hydrogenation catalyst are essential factors for the degree of signal enhancement.

Nuclear magnetic resonance (NMR) spectroscopy is one of the most powerful analytical tools for structural investigations of biomolecules and their interaction with therapeutically relevant ligands or drugs.<sup>[1]</sup> However, the major limitation narrowing the scope of NMR analysis is the inherent low sensitivity of this technique. In particular, upon binding of ligands to macromolecular targets, strong background signals often become the bottleneck for the interpretation of NMR spectra. In recent years, the application of hyperpolarization techniques, such as dynamic nuclear polarization (DNP),<sup>[2]</sup> chemically induced dynamic nuclear polarization (CIDNP),<sup>[3]</sup> hyperpolarized Xenon biosensors (HP/Xe),<sup>[4]</sup> parahydrogen-induced polarization (PHIP),<sup>[5]</sup> and the related SABRE<sup>[6]</sup> technique have been recognized as the most promising strategies to solve this problem. These approaches are based on the transfer of spin polarization from a highly polarized spin species to the nuclei of interest<sup>[6–7]</sup> or on direct examination of hyperpolarized nuclei<sup>[4]</sup> and result in a dramatic increase in signal strength compared to that present at thermal equilibrium.

A major advantage of the PHIP methodology is that no sophisticated and expensive equipment is required to induce hyperpolarization.<sup>[8]</sup> Nevertheless, only a surprisingly small number of simple biorelated molecules have been studied to date using this hyperpolarization method.<sup>[9]</sup> This is mainly due to the fact that an unsaturated moiety, which can be efficiently hydrogenated with the *p*-H<sub>2</sub> in a pairwise manner within the lifetime of the hyperpolarized species, must be present in the molecule of interest. This can be achieved through the introduction of an unsaturated building block acting as a PHIP label. However, the character and position of this PHIP label must be chosen carefully to ensure strong hyperpolarization and prevent conformational changes thus preserving bioactivity.<sup>[7c,9a,f,10]</sup>

Recently, we have introduced L-propargylglycine (Pra) (Figure 1b, **1**) as a building block for the study of PHIP in

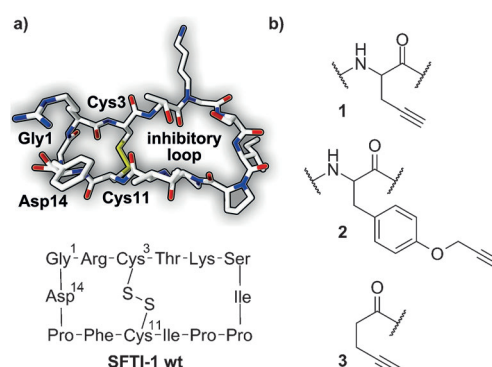


**Figure 1.** a) Structure of SFTI-1; lower panel: in three-letter code (disulfide bond exposed); upper panel: as a stick representation (blue N, red O, yellow S, white C, hydrogen left out for clarity). b) Chemical structures of PHIP labels L-propargylglycine (Pra, **1**), O-propargyl-L-tyrosine (**2**), and 4-pentynoic acid (**3**).

small synthetic linear and cyclic oligopeptides.<sup>[9e]</sup> This label can be easily introduced at each desired position of the peptide chain, needs no protection, and enables good signal enhancement. Encouraged by this outcome, we expanded this strategy to a constrained peptidic framework of the sunflower trypsin inhibitor-1 (SFTI-1, Figure 1).<sup>[11]</sup> This tetra-decapeptide, recently used for the development of novel tumor diagnostics and treatment tools, possesses a unique architecture comprising the head-to-tail peptidic macrocycle, the *cis*-amide, and the intramolecular disulfide bond between Cys<sup>3</sup> and Cys<sup>11</sup>.<sup>[11e,12]</sup>

As potential PHIP labels, the compounds **1–3** were chosen (Figure 1b), because they combine several crucial structural

[\*] G. Sauer,<sup>[‡]</sup> Dr. D. Tietze, Dr. T. Gutmann, Prof. Dr. G. Buntkowsky  
Eduard-Zintl-Institut für Anorganische und Physikalische Chemie  
Technische Universität Darmstadt  
Alarich-Weiss-Str. 4, 64287 Darmstadt (Germany)  
E-mail: tietze@chemie.tu-darmstadt.de  
Gerd.Buntkowsky@chemie.tu-darmstadt.de  
Homepage: <http://www.chemie.tu-darmstadt.de/buntkowsky/>  
D. Nasu,<sup>[‡]</sup> S. Englert, Dr. O. Avrutina, Prof. Dr. H. Kolmar  
Clemens-Schöpf-Institut für Organische Chemie und Biochemie  
Technische Universität Darmstadt  
Alarich-Weiss-Str. 4, 64287 Darmstadt (Germany)  
E-mail: Kolmar@Biochemie-TUD.de  
Homepage: <http://www.chemie.tu-darmstadt.de/kolmar>

[‡] These authors contributed equally to this work.

[\*\*] This research was supported by the Deutsche Forschungsgemeinschaft under contract Bu-911-22-1.

Supporting information for this article is available on the WWW under <http://dx.doi.org/10.1002/anie.201404668>.

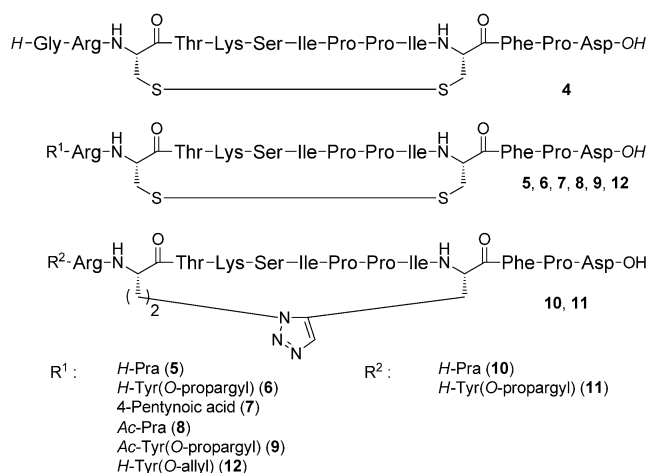


Figure 2. Chemical structures of 4–12.

and functional features. First, the alkyne groups provide significant inherent PHIP activity upon hydrogenation. Due to the fact that **1** has already demonstrated its utility as a hyperpolarizable moiety both when incorporated into small peptides and as an individual compound,<sup>[7c,9e]</sup> it was taken as a benchmark (Figure 2, peptide **5**).

The second important criterion was the accessibility of the triple bond to the homogeneous catalyst. Indeed, functional groups of peptidic backbone and side chains, such as -OH, -SH, -COOH, -CONH<sub>2</sub>, -NH<sub>2</sub>, and imidazole, could serve as coordination sites for the rhodium catalyst, thus reducing the hydrogenation efficacy or even poisoning the catalyst. Amide bonds as well as oxygen and sulfur species have been found to dramatically hinder PHIP.<sup>[9e]</sup> Therefore, the tyrosine derivative **2** should set the PHIP label further apart from the N-terminus, backbone, and functional groups (peptide **6**). 4-Pentynoic acid **3** featuring small size and the ability to cap the N-terminus of the peptide became another object of investigation (peptide **7**). Additionally, to prove the influence of the N-terminal amine peptides **8** and **9** with an acetylated N-terminus were synthesized.

The optimal site for the incorporation of the PHIP label was derived from the crystal structure of **4** in complex with trypsin (Figure 3, PDB 1SFI)<sup>[13]</sup> suggesting the N-terminal Gly<sup>1</sup> as an appropriate site for mutations (Figure 3).<sup>[14]</sup>

Since sulfur atoms within the disulfide bridges are strong electron donors and could therefore participate in the complexation with a rhodium catalyst,<sup>[15]</sup> thus affecting the hydrogenation, the intramolecular cystine motif was exchanged against its 1,5-disubstituted 1,2,3-triazolyl mimetic.<sup>[16]</sup>

As the bioactivity of the resulting construct is comparable to that of the parent all-natural peptide,<sup>[17]</sup> the peptidomimetics **10** and **11** were designed to study the influence of disulfide bonds on the PHIP efficacy while preserving the bioactivity.

Following the assembly of the linear precursors by microwave-assisted fluorenylmethyloxycarbonyl (Fmoc) solid-phase peptide synthesis (SPPS) and cleavage from the support, the air-mediated oxidative folding resulted in the disulfide-bridged peptides **5–9**. In peptidomimetics **10** and **11**,

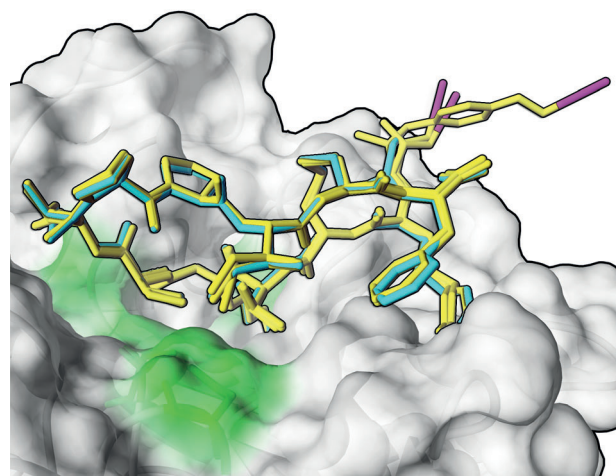


Figure 3. Structure and overlays of energy-minimized 3D models of SFTI-1 variants **4** (cyan),<sup>[13]</sup> **5**, **6**, **7** (yellow, acetylene groups are depicted in magenta, trypsin catalytic triad highlighted in green) as co-complex with trypsin to visualize the spatial position and orientation of the PHIP labels.

macrocyclization was achieved through the formation of a 1,5-disubstituted triazole through on-resin Ru<sup>II</sup>-catalyzed azide–alkyne cycloaddition (RuAAC)<sup>[17]</sup> (see the Supporting Information (SI) S4).

Subsequently, the <sup>1</sup>H hyperpolarization ability of individual building blocks Fmoc-L-Tyr(propargyl)-OH (Fmoc-**2**-OH) and pentynoic acid (**3**-OH) along with the compounds **5–12** were examined using Rh(dppb)(cod)BF<sub>4</sub>-catalyzed hydrogenation (cod = 1,5-cyclooctadien, dppb = 1,4-bis(diphenylphosphino)butane). Reactions were performed with approximately 50% para-H<sub>2</sub> enriched hydrogen at a pressure of 2 bar, which was generated using activated charcoal as catalyst at liquid nitrogen temperature.<sup>[18]</sup> After addition of *p*-H<sub>2</sub>, the reaction mixture was shaken for 10 s at terrestrial magnetic field and the sample was placed in the strong magnetic field of the spectrometer (7 Tesla). The hyperpolarized spectra were immediately detected using a single-scan experiment (45° excitation pulse). The signals of the product under thermal equilibrium, which are required for the calculation of the signal enhancement, were recorded employing multiple scans (typically 256 scans). The achieved signal enhancement (SE) was calculated as ratio of the integral of the hyperpolarized signal and the thermal equilibrium signal (see SI, S8). Additional hyperpolarized signals around 5.8, 2.2, and 1.5 ppm were caused by the hydrogenation of the cyclooctadienyl moiety of the catalyst.<sup>[19]</sup>

Hydrogenation of the triple bond of Fmoc-**2**-OH yielding the alkene-bearing Fmoc-L-Tyr(allyl)-OH led to hyperpolarized proton signals at 5.2–5.5 ppm with an SE of about 200. This enhancement is similar to that observed upon hydrogenation of Fmoc-L-propargylglycine (Fmoc-**1**-OH).<sup>[9e]</sup> Interestingly, the hydrogenation of pentynoic acid (**3**-OH) toward the respective pentenoic acid showed a 4.5 times higher signal enhancement (SE = 900) than that recorded for Fmoc-**1**-OH and Fmoc-**2**-OH. Signal enhancements for the second hydrogenation step resulting in the fully saturated products were usually very low or not observable (see SI, S9 T2). To

compare the SE for the examined compounds, the relaxation times  $T_1$  were measured for the protons of the newly formed  $\text{CH}_2$  ( $\text{H}^a/\text{H}^b$ ) group of the double bond (5.0–5.3 ppm, see SI, S9 T3). The highest  $T_1$  value was found for compound **3-OH**, which exhibited also the strongest signal enhancement.

For all SFTI-1 variants (**6–11**, Table 1) characteristic antiphase signals were observed, which were attributed to the presence of PHIP labels **1–3**. For peptide **5**, which

**Table 1:** Summary of calculated  $K_i$  and SE values for compounds **4–12**.

Entry	Label	Macrocytization	N-terminus	SE <sup>[a]</sup>	$K_i$ [nM] <sup>[b]</sup>
<b>4</b>	–	cystine	H-	–	$0.28 \pm 0.02$
<b>5</b>	<b>1</b>	cystine	H-	n.h.	$1.53 \pm 0.28$
<b>6</b>	<b>2</b>	cystine	H-	70	$1.41 \pm 0.27$
<b>6'</b>	<b>2</b>	cystine	H-	74	–
<b>6''</b>	<b>2</b>	cystine	H-	66	–
<b>7</b>	<b>3</b>	cystine	none	5	$0.20 \pm 0.03$
<b>8</b>	<b>1</b>	cystine	Ac-	n.h.	$0.21 \pm 0.04$
<b>8a</b>	<b>1</b>	–	Ac-	n.a.	–
<b>9</b>	<b>2</b>	cystine	Ac-	68	$0.21 \pm 0.03$
<b>9a</b>	<b>2</b>	–	Ac-	65	–
<b>10</b>	<b>1</b>	triazole	H-	n.a.	$7.21 \pm 0.90$
<b>11</b>	<b>2</b>	triazole	H-	35	$4.33 \pm 0.61$
<b>12</b>	<b>Tyr(O-allyl)</b>	cystine	H-	n.h.	$1.27 \pm 0.20$

[a] Values were calculated as described in SI (S8). [b] Error calculated by propagation of error for  $K_i^{\text{app}}$  and  $K_M$  (see SI, S5–S7). **6'** SE was studied in a water/ $[\text{D}_4]\text{MeOH}$  mixture (1:1, v/v) at 333 K; **6''** SE was studied in a water/ $[\text{D}_6]\text{ethanol}$  mixture (1:1, v/v) at 333 K; **8a** and **9a** are the reduced two-thiol peptides (see SI, S3); n.h. no hydrogenation was observed; n.a. not analyzable, product signals are negligibly small.

combined the Pra label with the free  $\alpha$ -amine and peptide **12**, no hydrogenation products were detected.

The highest SE of 70 observed in this study was detected for the propargyltyrosine-labeled peptide **6**. Figure 4 exemplarily shows  $^1\text{H}$  NMR spectra of peptide **6** upon hydrogenation with para-enriched hydrogen.

The  $^1\text{H}$   $T_1$  time of the resulting  $\text{CH}_2$  ( $\text{H}^a/\text{H}^b$ ) group in peptide **6** is 2.8 s. In contrast, only a weak enhancement was found for peptide **7**, although the  $^1\text{H}$   $T_1$  time of the  $\text{CH}_2$  group is within the same range (2.5 s). This is rather surprising

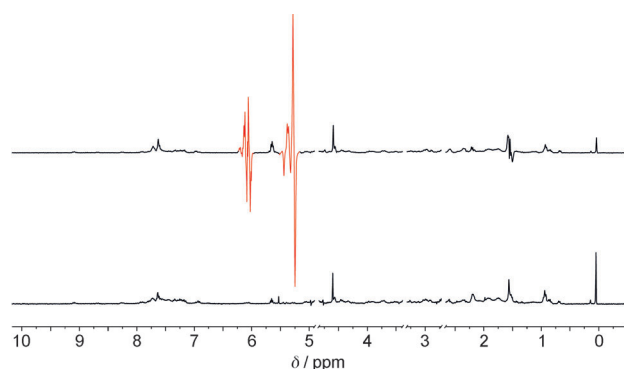


**Figure 4.** Top:  $^1\text{H}$  NMR spectrum of the reaction mixture comprising **6** and  $\text{Rh}(\text{cod})(\text{dppb})\text{BF}_4$  in  $[\text{D}_4]\text{MeOH}$ , recorded ca. 34 s after hydrogenation with para-enriched hydrogen. Hyperpolarized  $^1\text{H}$  signal from **6** highlighted in red. Bottom:  $^1\text{H}$  NMR spectrum recorded after relaxation of polarized spin states.

because unbound pentynoic acid (**3-OH**) showed the highest SE and longest relaxation time  $T_1$ . Due to the fact that  $T_1$  times for the examined compounds are all of the same order of magnitude, we suppose that such dramatic differences between the signal enhancements observed for the individual building blocks and their respective SFTI-bound derivatives cannot be explained only by the relaxation behavior of the spin states. Instead the rate of substrate hydrogenation within the Rh-catalyzed reaction cycle must determine the degree of signal enhancement. On the one hand, the hydrogenation process includes the binding of  $\text{H}_2$  at the Rh center to yield a dihydrido complex, followed by migratory insertion of H atoms at the unsaturated bonds and, on the other hand, the coordination of the respective multiple bond with the catalyst is a complex kinetic process. This suggests that the degree of signal enhancement depends on  $T_1$  relaxation, hydride transfer between the unsaturated moiety and the metal ion, and competition with the coordination sites of biomolecules.

As the free N-terminus could provide a suitable coordination site for the catalyst, acetylated peptides **8** and **9** were synthesized. Characteristic but very weak antiphase signals were detected for the Pra-labeled peptide **8**. The N-terminally capped peptide **9** displayed a residual SE of 68 similar to that for the nonacetylated variant **6**. Surprisingly, incorporation of pentynoic acid, which lacks an N-terminal functional group, led to a moderate SE of about 5 for peptide **7** indicating that N-terminal capping is not required for good signal enhancement.

In good agreement with the results obtained for the corresponding cystine-bridged counterparts **5** and **6**, the propargyltyrosine-labeled construct **11** showed significantly stronger SE compared to the respective Pra-bearing peptidomimetic **10**. Surprisingly, the SE for **11** was decreased by a factor of two compared to that of **6** containing an intramolecular disulfide bond. Therefore, we conclude that the triazolyl moiety affects the hydrogenation process, probably due to the competing coordination of the triazolyl moiety with the Rh-catalyst through the free electron pair on nitrogen. Since the highest SE were observed for the sulfur-containing derivatives **6**, **9**, and **9a** (the reduced two-thiol peptide; see SI, S3), their sulfur-bearing motifs have no pronounced influence on the coordination with the catalyst, which could be, however, attributed to the particular architecture of the investigated constructs.

Due to the potential biocompatibility problems associated with the usage of organic solvents, we conducted PHIP experiments in aqueous systems, namely, water/methanol and water/ethanol (1:1 v/v; see SI, S8 and S15), which required enhanced temperature to maintain the catalyst's activity (data not shown). At 333 K, the SE for **6** was 74 in water/MeOH, and 66 in water/EtOH, which is in the range of experiments in neat methanol. Under these conditions, the structural integrity of **6**, and hence its activity was not deteriorated (see SI, S26).<sup>[20]</sup>

Generally, our results suggest that functional groups in vicinity to the triple bond from the PHIP label limit the attainable signal enhancement as they can act as ligands coordinating to the hydrogenation catalyst. Hence, two factors must be considered to achieve pronounced signal



enhancement: 1) the accessibility of the triple bond within the catalytic cycle, and 2) its spatial remoteness from the peptide backbone.

To study the influence of the PHIP labels on the function of inhibitors **5–12**, their bioactivity was determined in kinetic studies using bovine trypsin and Boc-Gln-Ala-Arg-4-nitro-anilide (BOC = *tert*-butoxycarbonyl) as a chromogenic substrate (see SI, S5–S7).<sup>[16e,17,21]</sup> The substrate-independent inhibitory constants  $K_i$  of compounds **5–12** were calculated (Table 1) and displayed  $K_i$  values in the single-digit and subnanomolar range. The peptides **7**, **8**, and **9** lacking a free N-terminus displayed better inhibitory potency than **5** and **6** bearing an N-terminal amine; this corroborates the reported data on the bioactivity of SFTI constructs.<sup>[12b,22]</sup> The in silico model (Figure 3) shows that the side chain of **2** does not interfere with the binding site of the enzyme. Therefore, the bioactivity of the investigated compounds is not affected by the label and they all show  $K_i$  in the range of tight-binding inhibitors.

For the first time, parahydrogen-induced polarization was studied in bioactive peptidic frameworks bearing pendant terminal alkynes that were introduced through the PHIP labels comprising L-propargylglycine (**1**), O-propargyl-L-tyrosine (**2**), and 4-pentynoic acid (**3**). Exhibiting strong signal enhancements (SE = 200–900) and having only minor effects on the bioactivity of synthetic protease inhibitors, these labels allowed to reach significant signal enhancement in <sup>1</sup>H NMR spectra (SE up to 70). Acylation of the free amine terminus had no effect on the hyperpolarization ability, whereas replacement of the disulfide bridge through a 1,2,3-triazolyl moiety lowered the SE by a factor of two, probably due to the coordination with the rhodium catalyst.

While the observed signal enhancement is high, the measured  $T_1$  times are short. A straightforward strategy for  $T_1$  times extension is transferring the hyperpolarized nuclear spin order into long-lived nuclear singlet states as shown by Levitt<sup>[23]</sup> or through a polarization transfer to neighboring heteroatoms such as <sup>13</sup>C.<sup>[24]</sup> Alternatively, single-shot MR imaging on hyperpolarized samples with fast detection<sup>[25]</sup> or constant generation of hyperpolarization<sup>[26]</sup> could be applied for 2D NMR experiments aimed at investigating protein-ligand studies.

Our results indicate that  $T_1$  times of the hyperpolarized protons cannot serve as the only rationale for the observed differences in SE. We assume that the isolated spatial location of the triple bond and its accessibility for the hydrogenation catalyst are determining factors for the degree of signal enhancement. Indeed, the SE in the series of PHIP-labeled SFTI variants increased according to the length of alkyne-bearing arms that separate the triple bond from the peptide functional groups getting its maximal value for the longest O-propargyl-L-tyrosine derivative.

To the best of our knowledge, this is the first report on a systematic study of a diversely functionalized bioactive peptide by PHIP. It can be assumed that the propargyltyrosine residue may find general application as an efficient, structurally low invasive building block to selectively access PHIP in bioactive peptides, and in particular in aqueous systems. We suppose that our approach can be applied to a vast number of

biomolecular constructs. Moreover, as SFTI derivatives<sup>[11a,f]</sup> are potent inhibitors of tumor-associated proteases, PHIP labeling can open new avenues in magnetic resonance imaging.

Received: April 24, 2014

Revised: July 29, 2014

Published online: October 8, 2014

**Keywords:** inhibitors · NMR spectroscopy · nuclear spin hyperpolarization · PHIP · signal enhancement

- [1] a) P. J. Hajduk, R. P. Meadows, S. W. Fesik, *Q. Rev. Biophys.* **1999**, 32, 211–240; b) M. Pellecchia, D. S. Sem, K. Wuthrich, *Nat. Rev. Drug Discovery* **2002**, 1, 211–219; c) Y. Lee, H. Zeng, A. Mazur, M. Wegstroth, T. Carlomagno, M. Reese, D. Lee, S. Becker, C. Griesinger, C. Hilty, *Angew. Chem. Int. Ed.* **2012**, 51, 5179–5182; *Angew. Chem.* **2012**, 124, 5269–5272.
- [2] a) A. W. Overhauser, *Phys. Rev. Lett.* **1953**, 92, 411–415; b) R. A. Wind, J.-H. Ardenkjær-Larsen, *J. Magn. Reson.* **1999**, 141, 347–354; c) J. Ardenkjær-Larsen, S. Macholl, H. Jóhannesson, *Appl. Magn. Reson.* **2008**, 34, 509–522.
- [3] a) J. Bargon, H. Fischer, *Z. Naturforsch. A* **1967**, 22, 1556–1562; b) L. Kuhn in *Topics in Current Chemistry*, Vol. 338 (Ed.: L. T. Kuhn), Springer, Berlin **2013**, pp. 229–300; c) J. H. Lee, Y. Okuno, S. Cavagnero, *J. Magn. Reson.* **2014**, 241, 18–31.
- [4] M. M. Spence, S. M. Rubin, I. E. Dimitrov, E. J. Ruiz, D. E. Wemmer, A. Pines, S. Q. Yao, F. Tian, P. G. Schultz, *Proc. Natl. Acad. Sci. USA* **2001**, 98, 10654–10657.
- [5] a) T. C. Eisenschmid, R. U. Kirss, P. P. Deutsch, S. I. Hommeltoft, R. Eisenberg, J. Bargon, R. G. Lawler, A. L. Balch, *J. Am. Chem. Soc.* **1987**, 109, 8089–8091; b) C. R. Bowers, D. P. Weitekamp, *J. Am. Chem. Soc.* **1987**, 109, 5541–5542; c) M. G. Pravica, D. P. Weitekamp, *Chem. Phys. Lett.* **1988**, 145, 255–258.
- [6] R. W. Adams, J. A. Aguilar, K. D. Atkinson, M. J. Cowley, P. I. Elliott, S. B. Duckett, G. G. Green, I. G. Khazal, J. Lopez-Serrano, D. C. Williamson, *Science* **2009**, 323, 1708–1711.
- [7] a) T. Gutmann, T. Ratajczyk, S. Dillenberger, Y. Xu, A. Grünberg, H. Breitzke, U. Bommerich, T. Trantzsche, J. Bernarding, G. Buntkowsky, *Solid State Nucl. Magn. Reson.* **2011**, 40, 88–90; b) A. Thomas, M. Haake, F. W. Grevels, J. Bargon, *Angew. Chem. Int. Ed. Engl.* **1994**, 33, 755–757; *Angew. Chem.* **1994**, 106, 820–822; c) T. Trantzsche, J. Bernarding, M. Plaumann, D. Lego, T. Gutmann, T. Ratajczyk, S. Dillenberger, G. Buntkowsky, J. Bargon, U. Bommerich, *Phys. Chem. Chem. Phys.* **2012**, 14, 5601–5604.
- [8] I. V. Koptug, *Mendeleev Commun.* **2013**, 23, 299–312.
- [9] a) S. Aime, W. Dastru, R. Gobetto, A. Viale, *Org. Biomol. Chem.* **2005**, 3, 3948–3954; b) S. Glöggler, J. Colell, S. Appelt, *J. Magn. Reson.* **2013**, 235, 130–142; c) S. Glöggler, R. Muller, J. Colell, M. Emondts, M. Dabrowski, B. Blumich, S. Appelt, *Phys. Chem. Chem. Phys.* **2011**, 13, 13759–13764; d) J. B. Hovener, N. Schwaderlapp, T. Lickert, S. B. Duckett, R. E. Mewis, L. A. Highton, S. M. Kenny, G. G. Green, D. Leibfritz, J. G. Korvink, J. Hennig, D. von Elverfeldt, *Nat. Commun.* **2013**, 4, 2946; e) M. Körner, G. Sauer, A. Heil, D. Nasu, M. Empting, D. Tietze, S. Voigt, H. Weidler, T. Gutmann, O. Avrutina, H. Kolmar, T. Ratajczyk, G. Buntkowsky, *Chem. Commun.* **2013**, 49, 7839–7841; f) F. Reineri, D. Santelia, A. Viale, E. Cerutti, L. Poggi, T. Tichy, S. S. D. Premkumar, R. Gobetto, S. Aime, *J. Am. Chem. Soc.* **2010**, 132, 7186–7193; g) M. Roth, A. Koch, P. Kindervater, J. Bargon, H. W. Spiess, K. Münnemann, *J. Magn. Reson.* **2010**, 204, 50–55; h) P. C. Soon, X. Xu, B. Y. Zhang, F. Gruppi, J. W. Canary, A. Jerschow, *Chem. Commun.* **2013**, 49, 5304–5306; i) F. Gruppi, X. Xu, B. Y. Zhang, J. A. Tang, A. Jerschow, J. W.

- Canary, *Angew. Chem. Int. Ed.* **2012**, *51*, 11787–11790; *Angew. Chem.* **2012**, *124*, 11957–11960.
- [10] a) R. V. Shchepin, A. M. Coffey, K. W. Waddell, E. Y. Chekmenov, *J. Am. Chem. Soc.* **2012**, *134*, 3957–3960; b) R. V. Shchepin, E. Y. Chekmenov, *J. Labelled Compd. Radiopharm.* **2013**, *56*, 655–662.
- [11] a) H. Fittler, O. Avrutina, B. Glotzbach, M. Empting, H. Kolmar, *Org. Biomol. Chem.* **2013**, *11*, 1848–1857; b) M. L. Korsinczky, H. J. Schirra, D. J. Craik, *Curr. Protein Pept. Sci.* **2004**, *5*, 351–364; c) M. L. J. Korsinczky, H. J. Schirra, K. J. Rosengren, J. West, B. A. Condie, L. Otvos, M. A. Anderson, D. J. Craik, *J. Mol. Biol.* **2001**, *311*, 579–591; d) P. Li, S. Jiang, S.-L. Lee, C. Y. Lin, M. D. Johnson, R. B. Dickson, C. J. Michejda, P. P. Roller, *J. Med. Chem.* **2007**, *50*, 5976–5983; e) U. C. Marx, M. L. J. Korsinczky, H. J. Schirra, A. Jones, B. Condie, L. Otvos, D. J. Craik, *J. Biol. Chem.* **2003**, *278*, 21782–21789; f) H. Fittler, O. Avrutina, M. Empting, H. Kolmar, *J. Pept. Sci.* **2014**, *20*, 415–420.
- [12] a) M. L. Colgrave, M. J. Korsinczky, R. J. Clark, F. Foley, D. J. Craik, *Biopolymers* **2010**, *94*, 665–672; b) M. L. J. Korsinczky, R. J. Clark, D. J. Craik, *Biochemistry* **2005**, *44*, 1145–1153; c) J. D. McBride, E. M. Watson, A. B. E. Brauer, A. M. Jaulent, R. J. Leatherbarrow, *Pept. Sci.* **2002**, *66*, 79–92.
- [13] S. Luckett, R. S. Garcia, J. J. Barker, A. V. Konarev, P. R. Shewry, A. R. Clarke, R. L. Brady, *J. Mol. Biol.* **1999**, *290*, 525–533.
- [14] a) J. Austin, R. H. Kimura, Y. H. Woo, J. A. Camarero, *Amino Acids* **2010**, *38*, 1313–1322; b) N. L. Daly, Y. K. Chen, F. M. Foley, P. S. Bansal, R. Bharathi, R. J. Clark, C. P. Sommerhoff, D. J. Craik, *J. Biol. Chem.* **2006**, *281*, 23668–23675.
- [15] C. H. Bartholomew, P. K. Agrawal, J. R. Katzer in *Advances in Catalysis*, Vol. 31 (Eds.: H. P. D. D. Eley, B. W. Paul), Academic Press, New York, **1982**, pp. 135–242.
- [16] a) G. Appendino, S. Bacchiega, A. Minassi, M. G. Cascio, L. De Petrocellis, V. Di Marzo, *Angew. Chem. Int. Ed.* **2007**, *46*, 9312–9315; *Angew. Chem.* **2007**, *119*, 9472–9475; b) W. S. Horne, C. A. Olsen, J. M. Beierle, A. Montero, M. R. Ghadiri, *Angew. Chem. Int. Ed.* **2009**, *48*, 4718–4724; *Angew. Chem.* **2009**, *121*, 4812–4818; c) A. Tam, U. Arnold, M. B. Soellner, R. T. Raines, *J. Am. Chem. Soc.* **2007**, *129*, 12670–12671; d) D. Tietze, M. Tischler, S. Voigt, D. Imhof, O. Ohlenschläger, M. Görlach, G. Buntkowsky, *Chem. Eur. J.* **2010**, *16*, 7572–7578; e) M. Tischler, D. Nasu, M. Empting, S. Schmelz, D. W. Heinz, P. Rottmann, H. Kolmar, G. Buntkowsky, D. Tietze, O. Avrutina, *Angew. Chem. Int. Ed.* **2012**, *51*, 3708–3712; *Angew. Chem.* **2012**, *124*, 3768–3772.
- [17] M. Empting, O. Avrutina, R. Meusinger, S. Fabritz, M. Reinwarth, M. Biesalski, S. Voigt, G. Buntkowsky, H. Kolmar, *Angew. Chem. Int. Ed.* **2011**, *50*, 5207–5211; *Angew. Chem.* **2011**, *123*, 5313–5317.
- [18] T. Gutmann, M. Sellin, H. Breitzke, A. Stark, G. Buntkowsky, *Phys. Chem. Chem. Phys.* **2009**, *11*, 9170–9175.
- [19] S. Aime, D. Canet, W. Dastru, R. Gobetto, F. Reineri, A. Viale, *J. Phys. Chem. A* **2001**, *105*, 6305–6310.
- [20] a) L. M. Simon, M. Kotormán, A. Szabó, G. Garab, I. Laczkó, *Biochem. Biophys. Res. Commun.* **2004**, *317*, 610–613; b) P. D. Compton, R. J. Coll, A. L. Fink, *J. Biol. Chem.* **1986**, *261*, 1248–1252.
- [21] R. A. Copeland in *Evaluation of Enzyme Inhibitors in Drug Discovery*, Wiley, Hoboken, **2013**, pp. 245–285.
- [22] O. Avrutina, H. Fittler, B. Glotzbach, H. Kolmar, M. Empting, *Org. Biomol. Chem.* **2012**, *10*, 7753–7762.
- [23] M. H. Levitt, *Annu. Rev. Phys. Chem.* **2012**, *63*, 89–105.
- [24] L. Kuhn, J. Bargon in *In situ NMR Methods in Catalysis*, Vol. 276 (Eds.: J. Bargon, L. Kuhn), Springer Berlin, **2007**, pp. 25–68.
- [25] R. Schmidt, C. Laustsen, J. N. Dumez, M. I. Kettunen, E. M. Serrao, I. Marco-Rius, K. M. Brindle, J. H. Ardenkjaer-Larsen, L. Frydman, *J. Magn. Reson.* **2014**, *240*, 8–15.
- [26] M. Roth, P. Kindervater, H. P. Raich, J. Bargon, H. W. Spiess, K. Münnemann, *Angew. Chem. Int. Ed.* **2010**, *49*, 8358–8362; *Angew. Chem.* **2010**, *122*, 8536–8540.